Bioorganic & Medicinal Chemistry Letters 19 (2009) 5970–5974

Contents lists available at ScienceDirect

Bioorganic & Medicinal Chemistry Letters

journal homepage: www.elsevier.com/locate/bmcl

Structure based design of novel irreversible FAAH inhibitors

Jane L. Wang *, Scott J. Bowen, Barbara A. Schweitzer, Heather M. Madsen, Joseph McDonald, Matthew J. Pelc, Ruth E. Tenbrink, David Beidler, Atli Thorarensen

Pfizer Global Research and Development, 700 Chesterfield PKWY West, Chesterfield, MO 63017, USA

ARTICLE INFO

Article history:
Received 7 July 2009
Revised 17 July 2009
Accepted 22 July 2009
Available online 25 July 2009

Keywords:
Fatty acid amide hydrolase
FAAH
Endocannabinoid anandamide
Inflammation
Irreversible FAAH inhibitors

ABSTRACT

Fatty acid amide hydrolase (FAAH) has attracted significant attention due to its promise as an analgesic target. This has resulted in the discovery of numerous chemical classes as inhibitors of this potential therapeutic target. In this paper we disclose a new series of novel FAAH irreversible azetidine urea inhibitors. In general these compounds illustrate potent activity against the rat FAAH enzyme. Our SAR studies allowed us to optimize this series resulting in the identification of compounds **13** which were potent inhibitors of both human and rat enzyme. This series of compounds illustrated good hydrolase selectivity along with good PK properties.

The endocannabinoid system has been under intense scrutiny due to its multiple therapeutic implications.[1] Fatty acid amide hydrolase (FAAH) has been identified as an important regulator of signaling molecules in this complex pathway.[2] FAAH is an integral membrane protein that hydrolyzes bioactive amides, from the endocannabinoid anandamide and agonists of the peroxisome proliferator-activated receptors, such as *N*-oleoylethanolamine and *N*-palmitoylethanolamine, to free fatty acid and ethanolamine. Genetic or pharmacological inactivation of FAAH leads to analgesic, anti-inflammatory, anxiolytic, and anti-depressant phenotypes in rodents. This occurs without showing the undesirable side effects observed with direct cannabinoid receptor agonists. This indicates that FAAH represents an attractive therapeutic target for the treatment of pain, inflammation, and other central nervous system disorders. Several reversible and irreversible FAAH inhibitors have been reported including electrophilic ketones (e.g., OL-135) and carbamates (e.g., URB597), Figure 1.[3] A series of publications from Pfizer have detailed the optimization of piperidine/piperazine urea analogs resulting in the identification of PF-3845.[4] PF-3845 has illustrated potent in vivo analgesic effects correlating with inhibition of FAAH. These ureas inhibit FAAH by covalently modifying the enzyme's active site serine nucleophile and are completely selective for FAAH relative to other mammalian serine hydrolases. Optimization of irreversible inhibitors requires an alternative approach compared to optimization of reversible inhibitors.[5] In a seminal report from Pfizer, Ahn described the use of the second order rate constant k_{inact}/K_i as the appropriate way to describe inhibitor potency.[4a] Unlike IC_{50} values, k_{inact}/K_i values do not change with variable pre-incubation times and have been described as the best measure of potency for irreversible inhibitors.

In our ongoing chemistry program aimed at identifying potent inhibitors of FAAH, it was apparent that the unique properties possessed by PF-3845 (k_{inact}/K_i = 14,310 (M^{-1} s^{-1})) had to be incorporated in any new analog design. Our desire in expanding the chemical space of FAAH inhibitors was to explore what variations were tolerated as replacement of the piperidine ring system. The piperidine ring system was described as core structural motif in publications and patents from several companies. In this Letter, we describe the synthesis and structure–activity relationships (SAR) of a series of irreversible azetidine urea FAAH inhibitors.

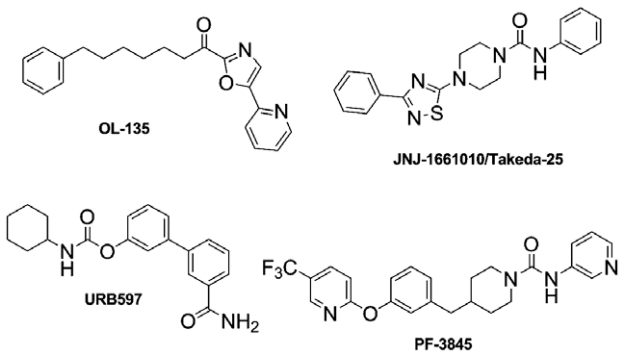

Figure 1. Structures of FAAH inhibitors.

* Corresponding author. Tel.: +1 636 247 5489; fax: +1 636 247 2086.
E-mail addresses: jane.l.wang@pfizer.com, j147wang@yahoo.com (J.L. Wang).

0960-894X/$ - see front matter © 2009 Elsevier Ltd. All rights reserved.
doi:10.1016/j.bmcl.2009.07.101

The availability of an X-ray structure of the piperidine analog, PF-3845, complexed to FAAH allowed us to visualize the structural requirements needed to design a replacement for the core piperidinyl moiety, while maintaining other key interactions. Covalently adducted FAAH-ligands were driven by key constraints. The position of the carbonyl moiety was critical because it made hydrogen bonds to several amide protons (residues 238–241) as part of the stabilization of transition state. At the distal end of the ligand, the 5-trifluoromethyl-pyridinyl moiety offered favorable potency and in vivo properties. The HetAr-O-Ph moiety of PF-3845 formed both aromatic and van der Waals contacts with the protein. Additionally, PF-3845 potency was likely also enhanced by conformational restriction which favored the bound conformer.

At the outset, a computational approach was utilized to assist in the evaluation of various linkers, to insure critical interactions were preserved, and that ligands were able to adopt a bound conformation with minimal strain. Shorter azetidine linkers (e.g., 2-carbon linker) reduced conformational flexibility, and were not able to make the same favorable distal interactions found in the reference structure, PF-3845. The longer linker required conformational strain to maintain both the distal interactions and positioning of the carbonyl moiety. The 3-carbon linker azetidines maintained critical interactions within the active site similar as the parent, PF-3845, Figure 2. This docking result convinced us to explore the 3-carbon linker azetidine as the replacement.

Our initial foray was the preparation of the model azetidine **6** with a 3-carbon linker, Scheme 1. Horner–Emmons olefination of compound **2**[6] with acetaldehyde **1**[7] provided compound **3** in 78% yield. Compound **3** was then deprotected in 98% yield and the resulting phenol was reacted with a range of electron deficient aryl halides forming the biaryl ethers **4a–d**. The Boc group was removed with TFA and the corresponding azetidines were treated with phenyl carbamates, which formed the ureas **5** in 40–86% yield.[4d] Hydrogenation of **5** with 10% Pd–C in MeOH obtained the key analogs **6a–d**. The olefin isomers were separated by SFC chromatography to provide pure geometrical isomers **5** *cis* and **5** *trans*.[8]

The initial small set of compounds **6a–d** probed our design by incorporating a fixed tail piece while modulating the aryl urea, Table 1. Selection of the aryl groups was dictated by previous experience.[4d] It was gratifying to find that the ureas **6a–d** inhibited FAAH activity. This data validated our design that the azetidine ring system was a viable replacement for the piperidine. We subsequently did further validation of our design by preparing compounds that had a shorter and a longer linker between the azetidine and the aryl group finding that the optimal linker was a 3-carbon spacer (data not shown).

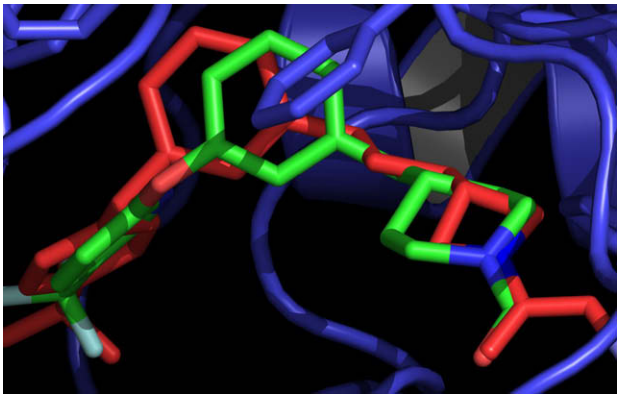

Figure 2. PF-3845 (green, X-ray), superimposed against model of compound **6** (red). Compounds were evaluated for strain using Schrodinger conformational search, by fixing the ligand covalently to Ser241, performing a conformational search within the active site using the OPLS force field, then performing a conformational search of the free ligand, and evaluating the relative potential energy difference.

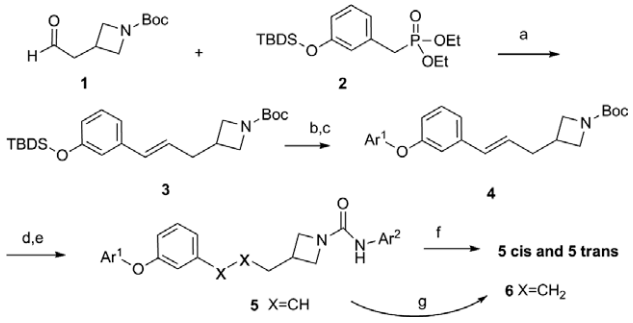

Scheme 1. Reagents and conditions: (a) K-OtBu, THF, −50 °C; (b) TBAF, THF; (c) Ar^1X, K_2CO_3, DMF; (d) TFA, CH_2Cl_2; (d) acetonitrile, DIEA, aryl phenylcarbamate; (f) SFC separation;[8] (g) H_2, 10% Pd–C, MeOH.

Table 1
Urea Heads effect on FAAH inhibition

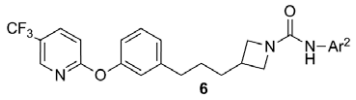

Compounds	Ar^2	*h* k_{inact}/K_i (M^{-1} s^{-1})	*r* k_{inact}/K_i (M^{-1} s^{-1})	clog *D*
6a		3030	1840	2.32
6b		1450	15300	3.97
6c		1090	688	3.54
6d	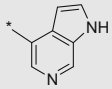	881	5160	3.21

Since compounds **6a–d** were prepared through intermediate **5**, we tested those intermediates as well. The analogs **5** were a mixture of olefin isomers, which displayed activity comparable to **6**. This allowed us to utilize **5** to rapidly explore variation of the tail and the urea in a library format. First we designed the library containing the tail pieces existing in **6a–d** and varied only urea heads. We found that only a very few aryl ureas were tolerated (data not shown). The second library focused on variation of the aryl ether tail pieces and incorporated only the pyridazine and the dimethylisoxazole as the aryl urea head. The SAR revealed that the human FAAH inhibitory potency was highly sensitive to tail pieces and only a few aryl groups tolerated, Figure 3a. These inhibitors all had in common with a 4-substituent in the tail. Although the striking structural differences in both tether length and size of ring system, azetidine analogs shared a very similar pattern, which was identified for the piperidine ureas.[4c] We evaluated the compounds against both human and rat FAAH enzyme and in general, these azetidine inhibitors were more potent against the rat enzyme, Figure 3b. The analogs with pyridazine urea head displayed the best human FAAH inhibition (Fig. 3a, ●). On the other hand, analogs with the dimethyl oxazole compounds showed a preference for the rat FAAH over human FAAH enzyme (Fig. 3b, ●). This clearly illustrated that the FAAH isozyme selectivity could be modulated by the appropriate combination of head and tail.

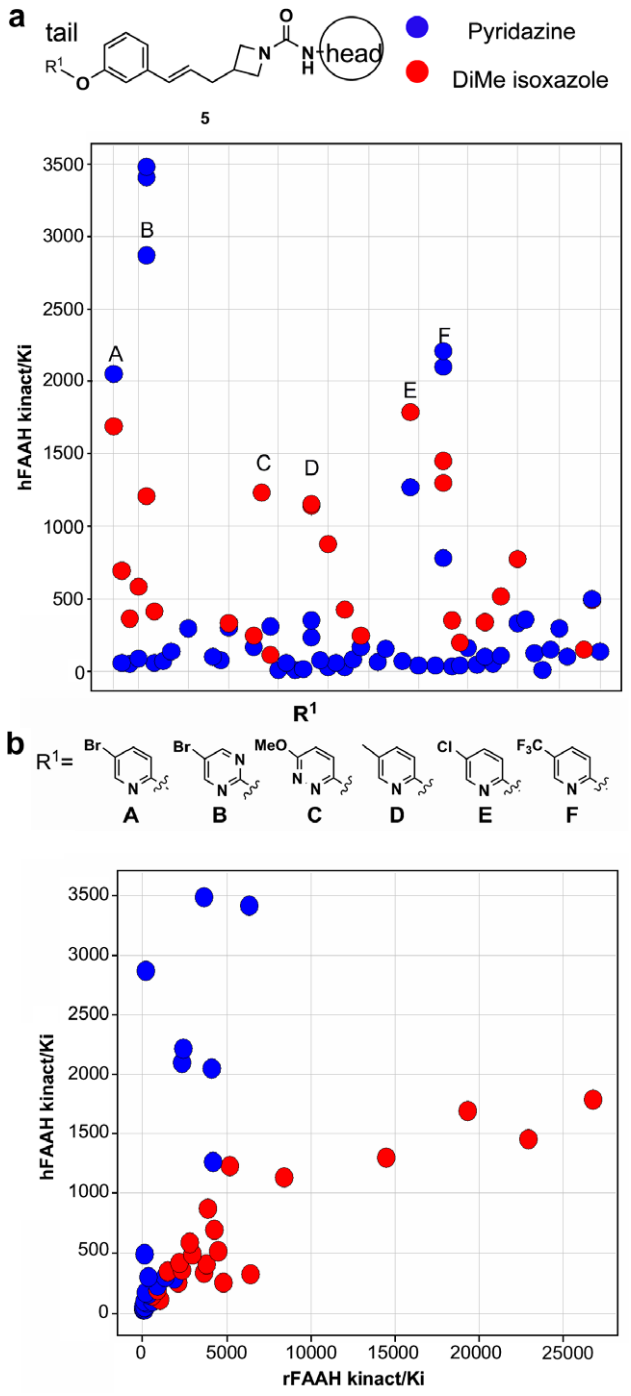

Figure 3. Illustrates SAR from libraries containing compounds of the generic structure **5**. (a) Tail pieces effect on human FAAH inhibition. (b) Human and rat enzyme activity correlated with the urea head being isoxazole versus pyridazine.

With demonstration of activity for the 3-carbon linked azetidine series, we sought to identify conformational restraints by further optimization of the scaffold, which might further improve the potency and the properties of these inhibitors. Modeling suggested that the saturated linker may occupy a predominantly transoid conformation, Figure 4. This transoid arrangement suggested an opportunity to explore added rigidity by systematically introducing *cis*- and *trans*-olefins into the linker. Introduction of a double bond into the 3-carbon linker was ideal because it was a simple form of restriction, and effectively probes the conformational requirements for the ligand. Introduction of double bonds was significantly easier to access than any ring constrained version.

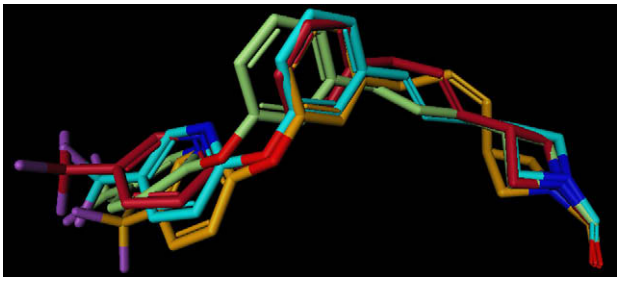

Figure 4. Superposition of conformationally optimized (covalently attached to Ser241) saturated (light green) 3-carbon linker **6a**, **5a** *trans* (light blue), **13a** *trans* (red), and **13a** *cis* (orange).

The olefin **13** was achieved from aldehyde **7** by reacting with carbon tetrabromide and triphenylphosphine providing the dibromoalkene **8**, Scheme 2. Selective mono-debromination of **8** was achieved with NH_4Cl, MeOH, and Zn dust to give the bromoalkene compound **9** in 48% yield. Compound **10**[9] in a mixture of THF and DMSO was added slowly to the activated Zn[10] at temperature below 65 °C. After removal of precipitates by filtration, the active benzylic-ZnCl reagent solution was then added to the mixture of **9** and Pd catalyst under argon conditions to form **12** as a mixture of olefin isomers. After deprotection of **12**, the intermediate was then reacted with phenyl carbamate to obtain desired compound **13**.

The final olefin **18** was prepared from aldehyde **14** by conversion to the alkene **15**, Scheme 3.[11] Subsequent hydroboration of alkene **15** followed by a Suzuki coupling with **16**[12] provided the desired key intermediate **17**. Deprotection and urea formation provided compound **18**.

The final analog elected to explore conformational space was the acetylene analog **21**, Scheme 4. This was achieved from benzylchloride **10**, which was converted to a benzyl bromide **19**. Compound **8** was treated with *n*-BuLi at −78 °C, followed by the slow addition of **19**, and the resulting mixture was stirred overnight at room temperature to afford the key intermediate **20**.[11] Simple functional group manipulation provided the desired product **21**.

The evaluation of all possible olefin regioisomers suggested that the location and the *cis* or *trans* disposition of the double bond were important to successful FAAH inhibition, Table 2. The double bond at position-2 provided analogs **13** with potent FAAH

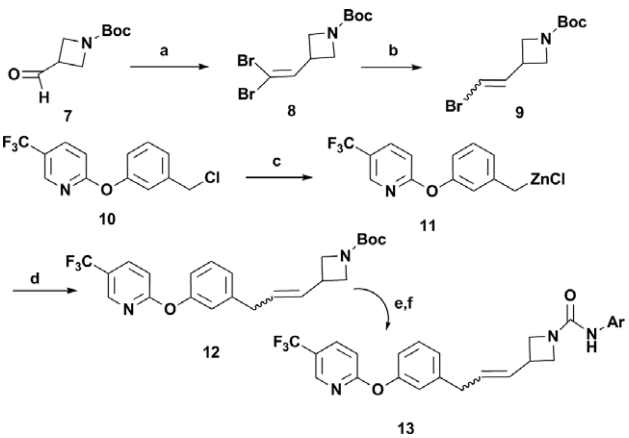

Scheme 2. Reagents and conditions: (a) PPh_3, CBr_4, CH_2Cl_2, yield 77%; (b) NH_4Cl, MeOH, THF, 0 °C 20 min then Zn, yield 48%; (c) Zn, TMSCl, 1,2-dibromoethane, DMSO, THF; (d) **9**, [1,1′-bis(diphenyl phosphino) ferrocene]dichloropalladium(II)methylene-chloride complex, CuI, yield 53%; (e) 2.5 equiv 4 M HCl in dioxane, yield 91%, CH_2Cl_2; (f) acetonitrile, DIEA, aryl phenylcarbamate, yield, 43%.

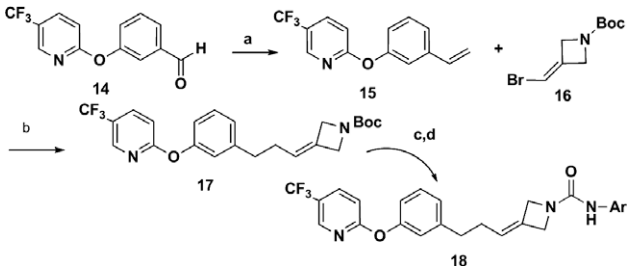

Scheme 3. Reagents and conditions: (a) methyltriphenylphosphonium-bromide, *n*-BuLi, THF, −78 °C, yield 26%; (b) 9-BBN, NaOH, Pd-tetrakis (triphenylphosphine), yield 91%; (c) 7.3 equiv TFA in CH_2Cl_2; (d) aryl phenylcarbamate acetonitrile, DIPEA.

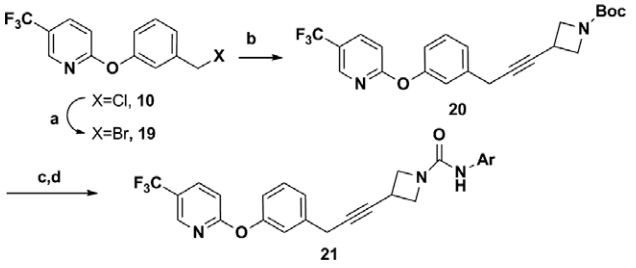

Scheme 4. Reagents and conditions: (a) acetone, LiBr, yield 100%; (b) **8**, *n*-BuLi, THF, −78 °C, yield 7%; (c) 2.5 equiv 4 M HCl in dioxane, CH_2Cl_2; (d) aryl phenylcarbamate, acetonitrile, DIEA.

Table 2
Effect of olefin location on FAAH inhibition

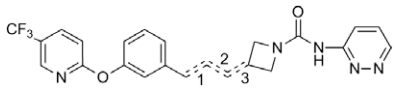

5, 6,13, 18, 21

Compounds	Linker	*h* k_{inact}/K_i (M^{-1} s^{-1})	*r* k_{inact}/K_i (M^{-1} s^{-1})	clog *D*
6a	Single	3030	1840	2.32
5 *cis*	Olefin-1	782	na	3.54
5 *trans*	Olefin-1	2100	2310	3.21
13 *cis*	Olefin-2	9000	5390	2.02
13 *trans*	Olefin-2	9340	2380	2.02
18	Olefin-3	621	1310	2.28
21	Propargyl-2	861	465	1.64

inhibition for both human and rat enzyme. Surprisingly, the stereochemistry of **13** seemed not to be sensitive to human FAAH inhibition (k_{inact}/K_i = 9000 and 9340 (M^{-1} s^{-1})), however there was some impact of the olefin stereochemistry for inhibition of rat FAAH. This was slightly unexpected, based upon the initial model of the saturated linker. However, the low energy bound conformer of **13** *cis* suggested that the *cis*-olefin was accommodated by way of an axial disposition relative to the azetidine, rather than equatorial, as suggested by **13** *trans* (see Fig. 4, red and orange). *Trans* **5** displayed similar potency for both human ($\sim k_{inact}/K_i$ = 2100 (M^{-1} s^{-1})) and rat (k_{inact}/K_i = 2310 (M^{-1} s^{-1})) FAAH inhibition, while **5** *cis* was a poor inhibitor. Comparing olefins at the 1- or 2- position, **5** *trans* rigidified the bond attached to the central aromatic ring as well as the double bond itself. In contrast, **13** *trans*, by virtue of its position as flanked by methylenes rigidified a smaller portion of the ligand. The slightly greater flexibility found in **13** *trans* relative to **5** *trans* allowed the ligand to adopt a more favored bound conformation. Conformational searching as described by the legend of Figure 2 suggested that the bound conformer of **5** *trans* was slightly more strained than **13** *trans*, compared to their respective free ligands

Table 3
Rat PK profile of selective compounds

Compd #	Cl (mL/min/kg)	*V* (L/kg)	$T_{1/2}$ (h)	BA (%)
13 *cis*	1.7	0.6	4.1	73
13 *trans*	11.1	1.8	2.2	93

(data not shown). Location of the olefin at position-3 (**18**) and propargyl-2 (**21**) led to poor potency for both human and rat FAAH. This SAR illustrated that incorporation of conformational constraint in the appropriate location in the 3-atom tether resulted in significant potency improvement compared to non-constrained analogs (Table 2).

The selectivity for other hydrolases was done in a comparable fashion as previously described.[4] The in vitro ABPP proteome profiling was done on both olefin isomers **13**. The selectivity profile observed for PF-3845 was retained in this new azetidine scaffold. We further evaluated the in vivo PK properties of the olefin **13** (Table 3). It was very gratifying to find that the olefin **13** had suitable PK properties in rat for further rat studies. The olefin **13** demonstrated low clearance (1.7 and 11.1 <30% rat liver blood flow) and high bioavailability (73% and 93%), but neither **13** *cis* nor **13** *trans* had comparable in vivo[13] efficacy to PF-3845, these data suggested that further optimization of azetidine would be required.[4c]

In summary, we have described the design of a novel scaffold, which replaced the piperidine of PF-3845 with 3-carbon linked azetidine. The azetidine compounds were potent inhibitors of both human and rat FAAH. The incorporation of a conformational restriction had significant effect on in vitro potency. Finally, the key properties of PF-3845 of high selectivity against other serine hydrolases and excellent PK were retained in the azetidine series. The preparation of ring constrained analogs that replace the olefin in the 3-carbon linker will be the subject of a future communication.

Acknowledgments

We would like to thank Prof. Benjamin F. Cravatt for his advice and extensive discussion on this project. J. Collins for chiral resolution and S. Yang for 2D NMR determination. In addition, T.K. Nomanbhoy at ActivX for ABPP proteome profiles; S. Wene for animal dosing and sample collection for PK analysis and R. Riley for bioanalytical method development, sample analysis, and pharmacokinetic analysis. Finally we would like to thank J. Rumsey for PK parameter assessment and L. Kirkovsky for PK discussions.

References and notes

1. (a) Lambert, D. M.; Fowler, C. J. *J. Med. Chem.* **2005**, *48*, 5059; (b) Pacher, P.; Batkai, S.; Kunos, G. *Pharmacol. Rev.* **2006**, *58*, 389; (c) Di Marzo, V. *Nat. Rev. Drug Disc.* **2008**, *7*, 438.
2. Ahn, K.; McKinney, M. K.; Cravatt, B. F. *Chem. Rev.* **2008**, *108*, 1687.
3. (a) Seierstad, M.; Breitenbucher, J. G. *J. Med. Chem.* **2008**, *51*, 7327; (b) Boger, D. L.; Miyauchi, H.; Du, W.; Hardouin, C.; Fecik, R. A.; Cheng, H.; Hwang, I.; Hedrick, M. P.; Leung, D.; Acevedo, O.; Guimaraes, C. R.; Jorgensen, W. L.; Cravatt, B. F. *J. Med. Chem.* **2005**, *48*, 1849.
4. (a) Ahn, K.; Johnson, D. S.; Fitzgerald, L. R.; Liimatta, M.; Arendse, A.; Stevenson, T.; Lund, E. T.; Nugent, R. A.; Nomanbhoy, T. K.; Alexander, J. P.; Cravatt, B. F. *Biochemistry* **2007**, *46*, 13019; (b) Mileni, M.; Johnson, D. S.; Wang, Z.; Everdeen, D. S.; Liimatta, M.; Pabst, B.; Bhattacharya, K.; Nugent, R. A.; Kamtekar, S.; Cravatt, B. F.; Ahn, K.; Stevens, R. C. *Proc. Natl. Acad. Sci. U.S.A.* **2008**, *105*, 12820; (c) Ahn, K.; Johnson, D. S.; Mileni, M.; Beidler, D.; Long, J. Z.; McKinney, M. K.; Weerpana, E.; Sadagopan, N.; Liimatta, M.; Smith, S. E.; Lazerwith, S.; Stiff, C.; Kamtekar, S.; Bhattacharya, K.; Zhang, Y.; Swaney, S.; Becelaere, K. V.; Stevens, R. C.; Cravatt, B. F. *Chem. Biol.* **2009**, *16*, 411–420; (d) Johnson, D. S.; Ahn, K.; Kesten, S.; Lazerwith, S. E.; Song, Y.; Morris, M.; Fay, L.; Gregory, T.; Stiff, C.; Dunbar, J. B.; Liimatta, M.; Beidler, D.; Smith, S.; Nomanbhoy, T. K.; Cravatt, B. F. *Bioorg. Med. Chem. Lett.* **2009**, *19*, 2865.
5. Copeland, R. A. *Enzymes: A practical introduction to structure, mechanism, and data analysis*, 2nd ed.; Wiley-VCH: New York, 2000. pp 318–349.
6. Compound **2** was prepared from 3-hydroxy methylbenzoate in four steps.

7. Matassa, V. G. WO 9318029 A1, 1993.
8. Olefin separation condition: Set up AI 30×250 mm chiral column elute with 20% EtOH and 80% CO2. Sample dissolved in 20 mL EtOH, 25 mg/mL, 1 mL per inject. The olefin stereochemistry was assigned by 2D NMR.
9. Compound **10** was prepared as described in WO 08047229, 2008.
10. Corley, E. G.; Conrad, K.; Murry, J. A.; Savarin, C.; Holko, J.; Boice, G. *J. Org. Chem.* **2004**, *69*, 5120.
11. Acharya, H. P.; Kobayashi, Y. *Tetrahedron* **2006**, *62*, 3329.
12. Compound **16** was prepared through the similar sequence as compound **9**.
13. The Pfizer Institutional Animal Care and Use Committee reviewed and approved the animal use in these studies. The animal care and use program is fully accredited by the Association for Assessment and Accreditation of Laboratory Animal Care, International.